



Cite this: *Chem. Commun.*, 2020, **56**, 2312

Received 23rd November 2019,  
Accepted 13th January 2020

DOI: 10.1039/c9cc09133e

[rsc.li/chemcomm](http://rsc.li/chemcomm)

GaN nanoparticles, 3–8 nm in diameter, are prepared by a microwave-assisted reaction of  $\text{GaCl}_3$  and  $\text{KNH}_2$  in ionic liquids. Instantaneously after the liquid-phase synthesis, the  $\beta$ -GaN nanoparticles are single-crystalline. The band gap is blue-shifted by 0.6 eV in comparison to bulk-GaN indicating quantum confinement effects. The GaN nanoparticles show intense green emission with a quantum yield of  $55 \pm 3\%$ .

Since the discovery of blue- and UV-light emitting diodes (LEDs), GaN has become one of the most important semiconductor materials.<sup>1</sup> Here, a technological breakthrough for GaN thin films was achieved by gas-phase deposition, which guarantees both high purity and high crystallinity.<sup>2</sup> The synthesis of nanoparticulate GaN is an even greater challenge compared to thin films, since the risk of contamination is even higher due to the large surface area of the nanoparticles and the associated high reactivity. In addition, nanoparticles are typically excluded from crystallization at high temperature ( $\geq 400$  °C) as they then naturally show uncontrolled growth and aggregation. High-quality GaN nanoparticles are nevertheless highly requested for optoelectronics (e.g., LEDs, lasers)<sup>3</sup> and catalysis (e.g., photocatalysis, electrocatalysis).<sup>4</sup>

In order to achieve high purity, high crystallinity and uniform particle size, GaN nanoparticles are mostly prepared using gas phase methods such as laser ablation deposition, chemical vapour deposition, thermal pyrolysis, or plasma pyrolysis.<sup>5</sup> Moreover, direct nitridation of gallium metal,<sup>6</sup> ammonolysis of oxide-containing starting materials (e.g.,  $\text{Ga}_2\text{O}_3$ ,  $\text{GaO(OH)}$ ,  $\text{Ga}(\text{NO}_3)_3$ ,  $\text{CO}(\text{NH}_2)_2$ )<sup>7</sup> or the thermal pyrolysis of nitrogen-rich molecular precursors (e.g.,  $\text{Ga}(\text{N}_3)_3$ ,  $\text{Ga}_2(\text{NMe}_2)_6$ )<sup>8</sup> in the gas phase and under supercritical conditions were applied.

<sup>a</sup> Institut für Anorganische Chemie, Karlsruhe Institute of Technology (KIT), Engesserstrasse 15, 76131 Karlsruhe, Germany. E-mail: claus.feldmann@kit.edu

<sup>b</sup> Laboratorium für Elektronenmikroskopie, Karlsruhe Institute of Technology (KIT), Engesserstrasse 7, 76131 Karlsruhe, Germany. E-mail: dagmar.gerthsen@kit.edu

† Electronic supplementary information (ESI) available: analytical equipment. See DOI: 10.1039/c9cc09133e

## Ionic-liquid-based synthesis of GaN nanoparticles<sup>†</sup>

Hannah F. Gaiser,<sup>a</sup> Radian Popescu,<sup>b</sup> Dagmar Gerthsen<sup>b</sup> and Claus Feldmann  <sup>\*</sup>a

The resulting GaN nanoparticles often suffer from broad size distribution and aggregation, low crystallinity and/or impurities that deteriorate the semiconductor properties due to undesired energy levels within the band gap.<sup>8,9</sup> High temperatures ( $> 400$  °C) and powder post-sintering are often required for crystallization and to obtain fluorescent GaN nanoparticles.<sup>6–8</sup> For liquid-phase synthesis of GaN nanoparticles thermolysis of  $\text{Ga}(\text{NH}_2)_3$  turned out to be promising and was performed in trioctylamine/hexadecylamine at 360 °C or by the reaction of  $\text{GaCl}_3$  and  $\text{LiN}(\text{SiMe}_3)_2$  with stearic acid as a stabilizer in octadecene at 280 °C to obtain  $\alpha$ -GaN.<sup>10</sup> Moreover, liquid-ammonia-based microemulsions were reported.<sup>11</sup> After liquid-phase synthesis, the emission intensity is typically limited and only visible under laser excitation<sup>10a</sup> or at low temperatures.<sup>10b,11</sup>

Aiming at the liquid-phase synthesis of GaN nanoparticles, we here suggest an ionic-liquid-based strategy,<sup>‡</sup> which results in well-crystallized  $\beta$ -GaN nanoparticles with a diameter of 3–8 nm showing intense green emission with a quantum yield of 55%. The synthesis strategy comprises two steps (Fig. 1). First of all,  $\text{GaCl}_3$  was dissolved in liquid  $\text{NH}_3$  at  $-35$  °C. Upon addition of  $\text{KNH}_2$  as a base, a colourless suspension of  $\text{Ga}(\text{NH}_2)_3$  was formed (Fig. 1a). After evaporation of all  $\text{NH}_3$  at room temperature, the

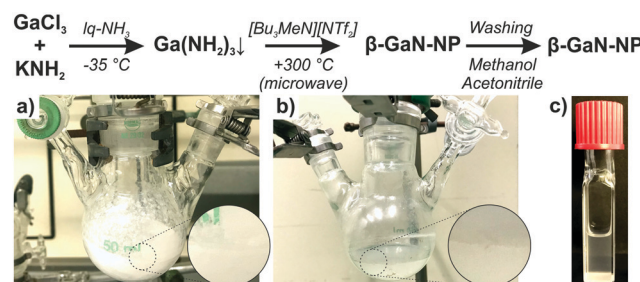


Fig. 1 Scheme illustrating the liquid-phase synthesis of  $\beta$ -GaN nanoparticles: (a) reaction of  $\text{GaCl}_3$  and  $\text{KNH}_2$  in liquid ammonia with precipitation of colourless  $\text{Ga}(\text{NH}_2)_3$ , (b) the almost transparent GaN suspension in ionic liquid after microwave heating, and (c) the  $\beta$ -GaN suspension after washing and redispersion in acetonitrile ( $0.2 \text{ mg mL}^{-1}$ ).



colourless solid was dispersed in  $[\text{Bu}_3\text{MeN}][\text{NTf}_2]$  as the ionic liquid ( $\text{Bu}_3\text{MeN}$ : tributylmethylammonium,  $\text{NTf}_2$ : bis(trifluoromethane)sulfonimide). In a second step, the resulting suspension of  $\text{Ga}(\text{NH}_2)_3$  in the ionic liquid was heated in a microwave oven for 1 hour to 300 °C (Fig. 1b). Finally, the colourless GaN nanoparticles were separated by centrifugation and purified by sequential redispersion/centrifugation in/from methanol and acetonitrile (Fig. 1c).

The synthesis strategy is characterized by  $\text{GaCl}_3$  as a most simple starting material and the strict exclusion of contaminants causing hydrolysis (*i.e.*  $\text{OH}/\text{H}_2\text{O}$  in starting materials, stabilizers, solvents, atmosphere).  $\text{KNH}_2$  is used as a base and amide source to obtain  $\text{Ga}(\text{NH}_2)_3$ . Microwave heating guarantees extremely fast heating and fast ammonolysis, especially at the beginning of the reaction. The ionic liquid stabilizes the GaN nanoparticles against uncontrolled growth and agglomeration. The high temperature (300 °C) in the aprotic ionic liquid supports the completion of the ammonolysis and evaporation of all  $\text{NH}_3$ . Ionic liquids, in this regard, were yet only used as inert electrolytes to gate semiconducting GaN thin films.<sup>5f,12</sup> For the synthesis of GaN, however, ionic liquids are here used for the first time. Finally, it needs to be noticed that the  $\text{Ga}(\text{NH}_2)_3$  intermediate is not nanosized (Fig. 1a). The rapid microwave-assisted decomposition with a significant loss of volume, however, supports the formation of GaN nanoparticles.

Particle size, particle shape and size distribution of the as-prepared GaN nanoparticles were determined by electron microscopy (Fig. 2). High-angle annular dark-field (HAADF) scanning transmission electron microscopy (STEM) overview

images and transmission electron microscopy (TEM) images show uniform nanoparticles with diameters of 3–8 nm (Fig. 2a and b). Moreover, high-resolution (HR)TEM images indicate parallel lattice fringes (Fig. 2c) that evidence the single-crystalline character of the as-prepared GaN. According to the observed lattice fringe distance of 2.2 Å, the structure of the nanoparticles is compatible with cubic sphalerite-type  $\beta$ -GaN (bulk- $\beta$ -GaN with  $d_{200} = 2.18$  Å).<sup>13</sup> The crystal structure of the  $\beta$ -GaN nanoparticles is also confirmed by two-dimensional (2D) Fourier transformation (FT) analysis (Fig. 2d), which is in accordance with the calculated diffraction pattern of bulk  $\beta$ -GaN in the [001] zone axis ( $Fm\bar{3}m$  with  $a = 3.985$  Å).<sup>13</sup>

Beside HRTEM and FT analysis, the presence and purity of the as-prepared GaN are confirmed by infrared spectroscopy (FT-IR) and energy-dispersive X-ray spectroscopy (EDXS). FT-IR spectra show the strongest absorption at 600–400  $\text{cm}^{-1}$ , which relates to the lattice vibration of crystalline GaN (Fig. 3a).<sup>14</sup> The weaker but similar shaped vibration at 1100–900  $\text{cm}^{-1}$  can be ascribed to a combination vibration. Further low-intensity vibrations at 2970–2880  $\text{cm}^{-1}$  ( $\nu(\text{C}-\text{H})$ ) and 1400–1200  $\text{cm}^{-1}$  ( $\nu(\text{S}=\text{O})$ ) relate to surface-adhered ionic liquid. The quantification of EDX spectra, recorded from bundles of GaN nanoparticles (Fig. 4), results in Ga and N contents of  $54 \pm 4$  and  $46 \pm 4$  at%, which is in fair agreement with the expectation (Ga and N with 50 at% each). According to EDXS element mappings, the as-prepared GaN shows uniform distribution of the elements (Ga and N) over the nanoparticle bundles (Fig. 4).

X-ray powder diffraction (XRD) analysis of the as-prepared GaN nanoparticles generally shows low scattering intensity. However, the broad peak centred at 35° of 2-Theta matches with the highest intensity peak of bulk- $\beta$ -GaN (Fig. 3b). The low

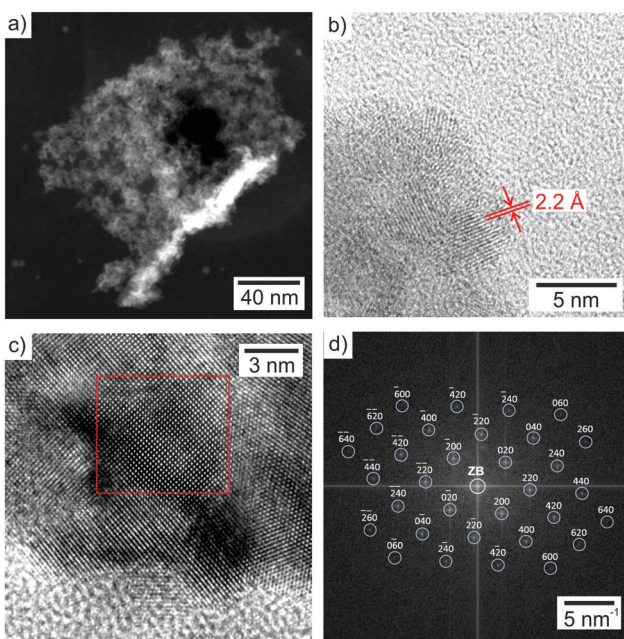


Fig. 2 Particle size, particle shape, and particle size distribution of the as-prepared GaN nanoparticles: (a) overview HAADF STEM image nanoparticles, (b) detailed TEM image of single-crystalline nanoparticles with lattice fringes, (c) HRTEM image with area for the 2D-FT analysis (red frame), (d) 2D-FT of the single-crystalline nanoparticle in (c) and calculated diffraction pattern with Miller indices for bulk- $\beta$ -GaN in the [001] zone axis (white circle indicates zero-order beam, ZB).

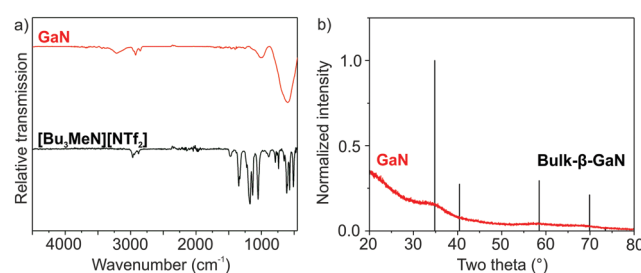


Fig. 3 FT-IR spectrum (a) and XRD (b) of the as-prepared GaN (FT-IR spectrum of the ionic liquid  $[\text{Bu}_3\text{MeN}][\text{NTf}_2]$  and XRD of bulk- $\beta$ -GaN (ICDD 088-2364) as references).

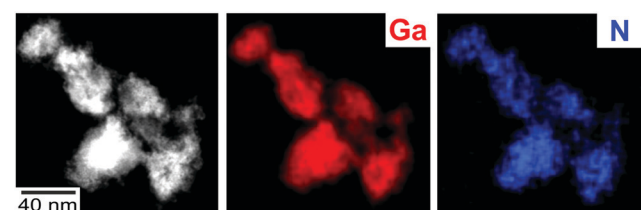


Fig. 4 HAADF STEM image of GaN nanoparticle bundles with EDXS elemental maps of Ga (red: based on  $\text{Ga}-\text{K}_{\alpha 1}$  line) and N (blue: based on  $\text{N}-\text{K}_{\alpha}$  line).



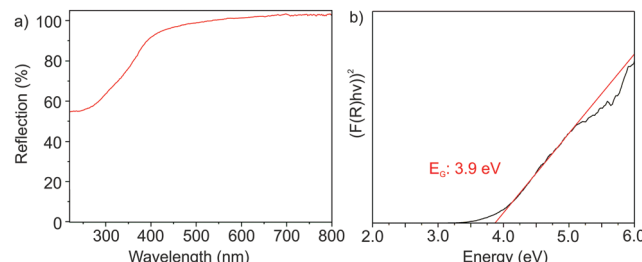


Fig. 5 Optical properties of the as-prepared GaN nanoparticles: (a) UV-Vis spectrum and (b) Tauc plot.

intensity and broad peak width, in fact, are to be expected taking the particle size of 3–8 nm into account. In regard of the slow solid-state diffusion in nitrides, all in all, the good crystallinity of GaN as confirmed by HRTEM, FT and XRD is surprising in view of the here applied liquid-phase synthesis with a maximum temperature of 300 °C. Typically, completion of the ammonolysis and nitride crystallization require temperatures of  $\geq 400$  °C.<sup>6–8</sup>

The optical properties of the as-prepared GaN nanoparticles were examined with UV-Vis spectroscopy (Fig. 5) and photoluminescence (PL) spectroscopy (Fig. 6). In this regard, UV-Vis spectra show a comparably steep absorption at 300–400 nm (Fig. 5a). By plotting  $(F(R)h\nu)^2$  versus  $(h\nu)$  in a Tauc plot, a band gap of 3.9 eV can be determined (Fig. 5b). The Tauc plot – as expected – indicates the nanomaterial to exhibit a direct band gap. In comparison to bulk- $\beta$ -GaN (3.3 eV),<sup>8a,b,15</sup> the band gap of the as-prepared nanoparticles is significantly blue-shifted by 0.6 eV, which can be ascribed to the small particle size, and which points to the presence of quantum-confinement effects.

Excitation spectra of the as-prepared GaN nanoparticles show strong absorption below 325 nm as well as a shoulder at 325–400 nm (Fig. 6a). Here, the strong absorption can be related to the band transition, whereas the shoulder indicates additional energy levels within the band gap. The strong band transition and the steep increase in absorption nevertheless point to the crystallinity of the as-prepared GaN, whereas the defect levels could relate from surface states. The width of the optical absorption observed in UV-Vis and excitation spectra (Fig. 5a and 6a) are narrower as compared to GaN nanoparticles that were post-synthesis sintered at  $\geq 400$  °C as powder samples.<sup>6–8</sup>

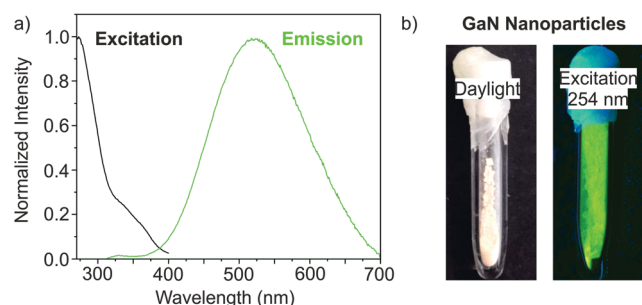


Fig. 6 Fluorescence properties of the as-prepared GaN nanoparticles: (a) excitation spectrum ( $\lambda_{\text{em}}: 523$  nm) and emission spectrum ( $\lambda_{\text{exc}}: 274$  nm); (b) GaN nanoparticle powder in daylight and under excitation ( $\lambda_{\text{exc}}: 254$  nm).

Emission spectra of the as-prepared GaN nanoparticles indicate strong fluorescence at 400 to 700 nm with its maximum at 523 nm (Fig. 6a). Direct conduction band-to-valence band emission is only observed with subordinate intensity at 325–400 nm. Consequently, the most relevant emission is located at lower energy than the band emission and can be related to donor–acceptor-type emission. The respective energy levels with wide dispersion may result from surface states as well as from gallium and/or nitrogen vacancies in the lattice. Qualitatively, the strong fluorescence is verified upon illumination using a UV lamp ( $\lambda_{\text{exc}}: 254$  nm) that results in a bright green emission (Fig. 6b). The strong emission was quantified by determining the absolute quantum yield following the method given by Friend *et al.*,<sup>16</sup> which results in a remarkable quantum yield of  $55 \pm 3\%$ . To our surprise, data on the fluorescence efficiency and quantum yield of liquid-phase-made GaN nanoparticles were not reported in the literature until now. A quantum yield of  $55 \pm 3\%$  for GaN nanoparticles – to the best of our knowledge – is achieved for the first time. This also impressively shows the effectiveness of the ionic-liquid-based synthesis strategy.

In conclusion, a synthesis strategy comprising the formation of a  $\text{Ga}(\text{NH}_2)_3$  intermediate in liquid ammonia followed by microwave-assisted heating in ionic liquids turned out to be successful to obtain GaN nanoparticles. Subsequent to liquid-phase synthesis, the as-prepared  $\beta$ -GaN nanoparticles are well-crystallized and exhibit particle diameters of 3–8 nm. The optical properties are characterized by a blue-shifted band gap of 3.9 eV, which is 0.6 eV above the band gap of bulk- $\beta$ -GaN. This finding can be related to quantum-confinement effects due to the small particle size. The GaN nanoparticles show strong absorption below 325 nm, which is in agreement with valence-band-to-conduction-band transition. Intense donor–acceptor-type green emission is observed at 400–700 nm (peaking at 523 nm) with an unprecedented quantum yield of  $55 \pm 3\%$ . Based on these results, the synthesis strategy will definitely be interesting also to prepare further metal nitrides.

The authors thank the Deutsche Forschungsgemeinschaft (DFG) for funding (NanoNitrid: FE911/10-1, GE 841/28-1).

## Conflicts of interest

There are no conflicts to declare.

## Notes and references

‡ Experimental: All experiments and purification procedures were performed under inert gas (argon), using standard Schlenk techniques or glove boxes. This also includes all centrifugation and washing procedures. Moreover, sample preparation and sample transfer for analytical characterization were strictly performed under inert conditions, *e.g.* by using specific transfer modules. Acetonitrile (Sigma-Aldrich, 99.5%) was refluxed over  $\text{CaH}_2$  onto  $\text{P}_4\text{O}_{10}$  and degassed by three freeze-pump-thaw cycles.  $\text{KNH}_2$  was synthesized by reacting potassium (Riedel-de-Haën, 99%) in liquid ammonia (Air Liquide, 99.98%) at  $-78$  °C using  $\text{Fe}_2\text{O}_3$  as a catalyst, followed by filtering and drying under vacuum. Gallium(III) chloride (ABCR, 99.999%) was used as purchased.  $[\text{Bu}_3\text{MeN}]^{\text{NTf}_2}$  was prepared according to literature procedures and dried for several days under reduced pressure ( $< 10^{-3}$  mbar) at  $230$  °C before use.<sup>17</sup>  $\beta$ -GaN nanoparticles: 88 mg of  $\text{GaCl}_3$  were dispersed in 15 mL of liquid ammonia at  $-35$  °C to obtain a colourless solution.



Thereafter, 83 mg  $\text{KNH}_2$  were added, which instantaneously results in the precipitation of colourless  $\text{Ga}(\text{NH}_2)_3$ . This mixture was stirred for an additional 10 minutes and then naturally warmed to room temperature. After evaporation of all  $\text{NH}_3$ , a voluminous, fluffy and colourless powder remained. This powder was dispersed in 15 mL of  $[\text{Bu}_3\text{MeN}][\text{NTf}_2]$  as ionic liquid. Subsequent to intense mixing, the suspension was rapidly heated (120 seconds) with a laboratory microwave oven (CEM MARS6) to 300 °C. This temperature was maintained for an additional 60 min. After natural cooling to room temperature, the resulting almost transparent and colourless suspension was diluted with 15 mL of acetonitrile. The as-prepared GaN nanoparticles were finally purified by centrifugation and redispersion in/from methanol and acetonitrile. The nanoparticles can be easily redispersed in acetonitrile or dried at room temperature under vacuum to obtain GaN powder samples.

- 1 S. Nakamura, *Science*, 1998, **281**, 956.
- 2 S. Nakamura, *Angew. Chem., Int. Ed.*, 2015, **54**, 7770.
- 3 (a) H. Alnoor, G. Pozina, V. Khranovskyy, X. Liu, D. Landolo, M. Willander and O. Nur, *J. Appl. Phys.*, 2016, **119**, 165702; (b) Y. C. Yao, J. M. Hwang, Z. P. Yang, J. Y. Huang, C. C. Lin, W. C. Shen, C. Y. Chou, M. T. Wang, C. Y. Huang, C. Y. Chen, M. T. Tsai, T. N. Lin, J. L. Shen and Y.-J. Lee, *Sci. Rep.*, 2016, **6**, 22659.
- 4 (a) Z. Wang, J. Han, Z. Li, M. Li, H. Wang, X. Zong and C. Li, *Adv. Energy Mater.*, 2016, **6**, 1600864; (b) B. AlOtaibi, S. Fan, D. Wang, J. Ye and Z. Mi, *ACS Catal.*, 2015, **5**, 5342; (c) S. Fan, B. AlOtaibi, S. Y. Woo, Y. Wang, G. A. Botton and Z. Mi, *Nano Lett.*, 2015, **15**, 2721.
- 5 (a) Y. H. Ji, R. Z. Wang, X. Y. Feng, Y. F. Zhang and H. Yan, *J. Phys. Chem. C*, 2017, **121**, 24804; (b) Z. S. Schiaber, G. Calabrese, X. Kong, A. Trampert, B. Jenichen, J. H. Dias da Silva, L. Geelhaar, O. Brandt and S. Fernandez-Garrido, *Nano Lett.*, 2017, **17**, 63; (c) A. Demirel, T. Oztas, C. Kursungoz, I. Yilmaz and B. Ortac, *J. Nanopart. Res.*, 2016, **18**, 1; (d) Y. Xu, B. Yao and Q. Cui, *RSC Adv.*, 2016, **6**, 7521; (e) B. Liu, B. Yang, F. Yuan, Q. Liu, D. Shi, C. Jiang, J. Zhang, T. Staedler and X. Jiang, *Nano Lett.*, 2015, **15**, 7837; (f) Z. Y. Chen, H. T. Yuan, X. Q. Wang, N. Ma, Y. W. Zhang, H. Shimotani, Z. X. Qin, B. Shen and Y. Iwasa, *Appl. Phys. Lett.*, 2013, **103**, 253508.
- 6 (a) G. A. Sapunov, A. D. Bolshakov, V. V. Fedorov, A. M. Mozharov, D. A. Kirilenko, A. A. Sitnikova and I. S. Mukhin, *J. Phys.*, 2018, **1038**, 012053; (b) C. Collado, G. Goglio, G. Demazeau, A. S. Barriere, L. Hirsch and M. Leroux, *Mater. Res. Bull.*, 2002, **37**, 841.
- 7 (a) M. Kumar, V. P. Singh, S. Dubey, Y. Suh and S. H. Park, *Opt. Mater.*, 2018, **75**, 61; (b) W. Lei, M. G. Willinger, M. Antonietti and C. Giordano, *Chem. – Eur. J.*, 2015, **21**, 18976; (c) N. F. Zhuang, X. Wang, F. Fei, C. C. Liu, L. Wei, Y. F. Zhang, X. L. Hu and J. Z. Chen, *J. Nanopart. Res.*, 2013, **15**, 1458.
- 8 (a) B. Giroire, S. Marre, A. Garcia, T. Cardinal and C. Aymonier, *React. Chem. Eng.*, 2016, **1**, 151; (b) B. Mazumder and A. L. Hector, *J. Mater. Chem.*, 2009, **19**, 4673; (c) A. C. Frank and R. A. Fischer, *Adv. Mater.*, 1998, **10**, 961.
- 9 A. Patsha, S. Amirthapandian, R. Pandian and S. Dhara, *J. Mater. Chem. C*, 2013, **1**, 8086.
- 10 (a) Y. C. Choi, H. Kim, C. Lee, J. Son, H. Baik, S. Park, J. Kim and K. S. Jeong, *Chem. Mater.*, 2019, **31**, 5370; (b) O. I. Micic, S. P. Ahrenkiel, D. Bertram and A. J. Nozik, *Appl. Phys. Lett.*, 1999, **75**, 478.
- 11 F. Gyger, P. Bockstaller, H. Gröger, D. Gerthsen and C. Feldmann, *Chem. Commun.*, 2014, **50**, 2939.
- 12 (a) A. Lahiri, N. Borisenko, A. Borodin and F. Endres, *Chem. Commun.*, 2014, **50**, 10438; (b) Q.-P. Li and B. Yan, *RSC Adv.*, 2012, **2**, 10840.
- 13 A. F. Wright and J. S. Nelson, *Phys. Rev. B: Condens. Matter Mater. Phys.*, 1995, **51**, 7866.
- 14 (a) G. Pan, M. E. Kordes and P. G. van Patten, *Chem. Mater.*, 2006, **18**, 3915; (b) A. S. Barker and M. Ilegems, *Phys. Rev.*, 1973, **7**, 743.
- 15 H. Morkoc, S. Strite, G. B. Gao, M. E. Lin, B. Sverdlov and M. Burns, *J. Appl. Phys.*, 1994, **76**, 1363.
- 16 J. C. de Mello, H. F. Wittmann and R. H. Friend, *Adv. Mater.*, 1997, **9**, 230.
- 17 T. Welton, *Chem. Rev.*, 1999, **99**, 2071.

